# We are IntechOpen, the world's leading publisher of Open Access books Built by scientists, for scientists

6,900
Open access books available

185,000
International authors and editors

200M
Downloads

Our authors are among the

154
Countries delivered to

TOP 1%
most cited scientists

12.2%
Contributors from top 500 universities

WEB OF SCIENCE™

Selection of our books indexed in the Book Citation Index in Web of Science™ Core Collection (BKCI)

Interested in publishing with us?
Contact book.department@intechopen.com

Numbers displayed above are based on latest data collected.
For more information visit www.intechopen.com

Chapter 3

# Continuous Casting of Thin Aluminum Strips Using the Electromagnetic Levitation

Marcela Pokusová

Additional information is available at the end of the chapter

http://dx.doi.org/10.5772/intechopen.70681

**Abstract**

In the development of the aluminum (Al) alloys continuous casting, the significant change was involved by replacing the mechanical contact between solidified molten metal and the mould's wall with the electromagnetic force action. Here, the function of the strip's surface shaping takes the special inductor known as the electromagnetic mould (EMM). The method for calculation the horizontal EMM's parameters for continuous casting of the thin strip from the Al alloys is presented. It is based on computing the distribution of the magnetic field using the interaction between an inductor and surface of the shaped molten metal. The operating frequency of alternating current passing through the inductor, which depends on the density, the surface tension, specific electric conductivity of the liquid metal, and the pool thickness, is determined. To shape the upper and bottom peripheries of the strip of 20 × 150 mm, the system of inductors was developed, and parameters for pouring of the AlSi8.5Cu and AlSn20 alloys were computed. The proposed EMM design considers the magnetic field distribution inside the inductor and the size of air gap between the liquid metal and inductor.

**Keywords:** aluminum alloys, strip, continuous casting, liquid metal, surface shaping, electromagnetic force, levitation

## 1. Introduction

Introducing the continuous casting of metal materials has made an increase in the productivity and quality of semi-products possible, but has also shown many shortcomings and reserves of this technology. In addition to the internal negative traits of the molten metal determined by the physical phenomena related to the solidification, in many materials, the surface defects occurring have already arisen in the mould—crystallizer itself, where the liquid metal has the mechanical contact with its walls. The friction forces between the solidified molten metal and crystallizer's walls cause the formation of the skin breakings or cracks, which damage the part

INTECH
open science | open minds

© 2017 The Author(s). Licensee InTech. This chapter is distributed under the terms of the Creative Commons Attribution License (http://creativecommons.org/licenses/by/3.0), which permits unrestricted use, distribution, and reproduction in any medium, provided the original work is properly cited.

of a surface and make harder the next processing, for example, rolling. Therefore, the research and development have focused firstly on the issue of improving ingots' surface quality. For the continuous casting technologies of the Al alloys, development has been initially concentrated on narrowing the zone, where the shaping of liquid metal occurs. However, the results achieved did not give satisfactory improvement in the surface quality.

An important milestone was reached in the development of continuous casting for aluminum alloys, with the substitution of the mechanical contact of the solidifying molten metal with the mould's walls for shaping a free surface, with the use of an electromagnetic force instead. The function of confining and shaping was taken over by a special coil—inductor known as an electromagnetic mould (EMM) [1]. The conventional vertical EMM has been successfully used on a slab section up to 1 $m^2$. Insights from the practice as well as theory have concurred that the vertical EMM is not suitable for continuous casting of the Al alloys semi-products with a cross section less than 0.01 $m^2$, and in particular for strips with a thickness of less than 25 mm [2]. Likewise, the laboratory testing of a conductive method for generating the levitation with the additional induction confining and shaping did not provide results which would justify the continuing development in this direction.

Today, when the trend is toward reducing the slab section and producing a near-net-shape product, horizontal electromagnetic casting can offer a solution to this problem [2]. Many studies have been conducted on the vertical EMM, focusing on free surface shaping [3–6], but only a small number of papers have been published on computing the parameters of horizontal EMM and determining their boundary values [7]. The EMM development has begun with the aim of replacing the technology of continuous casting of a 150 × 30 mm strip into a horizontal graphite mould from which the desired semi-product with a section of 150 × 20 mm, and without any surface defects was achieved by milling the 5 mm layer from each surface.

## 2. Horizontal electromagnetic mould

The development of an electromagnetic mould arranged horizontally began when it was discovered experimentally that as the molten metal approaches the mould, the value of the electromagnetic repelling force increases simultaneously. When the air gap is reduced from 5 to 0 mm, a steep increase in the repelling force ensures a steady positioning of the molten metal's surface to the inductor. In the early stages of investigation, the calculation of the parameters for the horizontal EMM (HEMM) started with the experimentally determined dependence of the air gap $a$ on the magnetic field intensity $H$. This was then transformed into a mathematical form using regression analysis [8]. In the next stage [9], increasing the pressure generated by the magnetic field when the air gap is reduced was explained as the result of interactions between the electrical current of the inductor and the conductive liquid metal. On this basis, the relations were formulated to compute the dependence of $a$-$H$ in the working space of a real inductor using the finite element method [10].

### 2.1. Interaction between magnetic field of a conductor and its mirror image

If a conductor, carrying an alternating current $I$, is getting closer to an electric conductive surface, the electric current is induced in this plane. Its intensity corresponds to the local

value of the magnetic field intensity, but it has an opposite sign. Here, the magnetic field and the spatial distribution of lines with the same value of the intensity $\boldsymbol{H}$ are determined by the interaction between this conductor and a fictitious one which is its mirror image below a plane which the magnetic field penetrates through, as it is shown in **Figure 1**.

Let us choose the conductor of a circular cross section with a radius $R$, which is passed by the electric current with a density $\boldsymbol{J}$. From Biot-Savart's law, it follows that in this single conductor, at any radius $r$ the circular magnetic field of intensity $\boldsymbol{H}_r$ induced by electric current $\boldsymbol{I}_r = \boldsymbol{J}\pi r^2$ will act, where

$$\boldsymbol{H}_r = \frac{\boldsymbol{I}_r}{2\pi r} = \frac{\boldsymbol{J}\pi r^2}{2\pi r} = \frac{\boldsymbol{J}r}{2} \tag{1}$$

In generating the magnetic field at the radius $r$, the only current $\boldsymbol{I}_r$ is involved which is passing through the surface enclosed by a circular vector $\boldsymbol{H}_r$, hence the current flowing in a cylindrical space with the radius from zero to $r$. The electric current passing through a circular ring between $R$ and $r$ is not involved in producing the magnetic field $\boldsymbol{H}_r$, because of the contribution of this area into the cylinder with radius $r$ is zero, where $\oint \boldsymbol{H} d\boldsymbol{s} = 0$. According to Eq. (1), at conductor's axis, the intensity of $\boldsymbol{H}_r$ is zero, and on its surface, since $r = R$, it is the highest. When the radius increases beyond conductor's contour, that is, $r > R$, the magnetic field is already produced by the current $\boldsymbol{I} = \boldsymbol{J}\pi R^2$, and the value of $\boldsymbol{H}_r$ is $\boldsymbol{H}_r = \boldsymbol{I}/2\pi R$. At any point on the connecting line of axes of both conductors, the magnetic field intensity in scalar form will be equal to a sum of contributions $H'$ and $H''$ from both conductors, and the course of total values $H = H' + H''$ is presented in **Figure 1a**. From **Figure 1a**, it follows that in the conductors at the distance $l''$, there are located points 1 and $1'$, at which the value of $H$ is zero, when

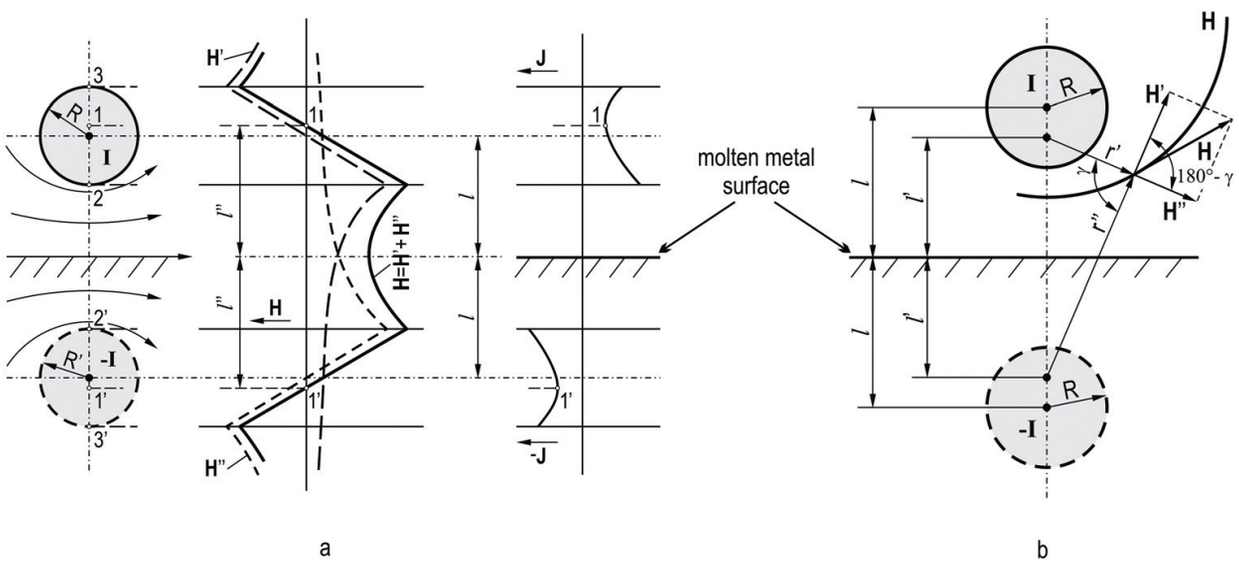


**Figure 1.** Interaction between the magnetic fields of a real conductor and its mirror image in a liquid metal: (a) distribution of current densities $\boldsymbol{J}$ and magnetic field intensities $\boldsymbol{H}$ on the connection line of axes of both conductors; (b) asymmetrical distribution of the magnetic field lines of force around a real conductor and its mirror image.

$$H = H' + H'' = 0 = \frac{J\left(l'' - l\right)}{2} - \frac{JR^2\pi}{2\pi\left(l'' + l\right)} = \frac{J\left(l'' - l\right)\left(l'' + l\right) - JR^2}{2\pi\left(l'' + l\right)} \tag{2}$$

The last term on the right side will be null if its numerator is null.

$$0 = J\left(l'' - l\right)\left(l'' + l\right) - JR^2 = l''^2 - l^2 - R^2 \text{ when } l''^2 = l^2 + R^2 \tag{3}$$

At the connection line of conductors' axis at the distances 1 and 1′, the density of electric current passing through the conductors will be also the lowest. At both conductors, the asymmetrical distribution of the magnetic field lines of force around inductor's conductor and its mirror image will cause an increase in the current density in the areas adjacent to a plane of the magnetic field penetration, and hence shifting the axes of symmetry of the electric current flowing on the value $l - l'$ toward each other (**Figure 1b**). From the position of points with the null intensity of $H$, using Eq. (3), we can calculate the distance of the axis of symmetry of the current flow in space [10–12].

$$l^2 = l'^2 + R^2 \tag{4}$$

At a general point of space determined by an intersection point of arcs of the circles with radii $r'$ and $r''$, the localized value $H$ is given by the contribution from both the conductors $H = H' + H''$. We can regard the components $H'$ and $H''$, defined by Eq. (1), as straight and lying in the tangent lines of circles in which the centers are in a joining line of conductors' centers at a distance $l'$ from a considered plane. According to **Figure 1b**, the absolute value $H$ can be calculated using the law of cosines.

$$H = \sqrt{H'^2 + H''^2 - 2H'H''\cos\gamma'} = \frac{2Il'}{\pi r'^2 r''^2} \tag{5}$$

The lines of a constant value $H$ are representing the distribution of the force lines of the magnetic field (a segment of one is plotted in **Figure 1b**), and they are sections of the equipotential surfaces through a plane perpendicular to conductors' axes, the real one and its mirror image. Because of between the conductor and its mirror image the magnetic field intensity is the sum of contributions $H = H' + H''$, the total value $H$ will be obviously higher than that one induced by a single conductor with the same flow of electric current on the same radius, and the highest value will be in a connecting line of their axes. Applying the iterative method to calculate the spatial distribution of the electric current and magnetic field intensities according to Sakane and others [4, 13, 14], without an intentional employing the mirroring, the values obtained under the model conditions are very close to those computed using Eqs. (1)–(5).

### 2.2. Calculation of magnetic field distribution in horizontal EMM

The method of HEMM design presented is based on the calculation of the magnetic field distribution, which is based on the interaction between the inductor and the surface of the

shaped molten metal. The condition of equilibrium between gravitational force and electromagnetic force in the HEMM can be defined according to the equation [3, 15]

$$\rho g h = \frac{\mu H^2}{4}, \text{ when } h = \frac{\mu H^2}{4\rho g} \tag{6}$$

where $h$ is the height of liquid metal (m), $\rho$ is the density of molten metal (kg m$^{-3}$), $H$ is the magnetic field intensity (A m$^{-1}$), and $\mu$ is the permeability of a medium, when $\mu \approx \mu_0 = 4\pi \times 10^{-7}$ H m$^{-1}$.

The analysis of the specific situation when the molten metal is brought closer to the inductor's face will be conducted with the inductor which has a cross section with an external central peak as shown in **Figure 2**.

As it was mentioned above, the interaction of fields of the inductor and its mirror image moves the centers of the electrical current flow closer together and increases the current density at the inductor's face adjacent to the liquid metal. In such a case, the conductor with radius $R$ through which the current $I$ passes, at a distance $l$ from the electric conductive face of the molten metal, will generate a magnetic field equal to the one generated by a conductor of zero thickness

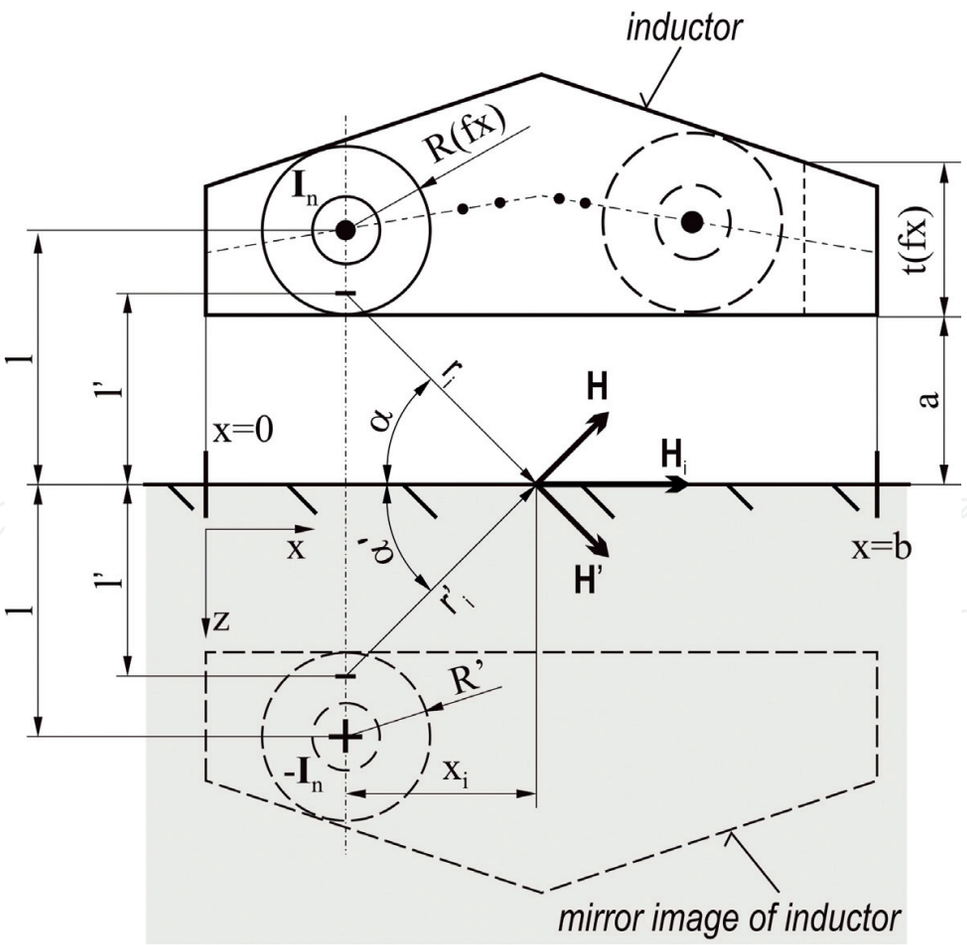


**Figure 2.** Inductor with a central peak.

having the values of the current $I$ the same, but at the distance of $l'$ from the surface different, that is, $l^2 = l'^2 + R^2$ according to Eq. (4). Then the magnetic field intensity $H_i$ on the molten metal surface will be the vector sum of both components from the conductor itself $H$ and from its mirroring image $H'$. If the inductor is at a distance $a$ from the liquid metal, when $l = a + R$, the addition of intensity $H_i$ from the selected element at a distance $x_i$ from the perpendicular to the surface will be

$$H_i = \frac{I}{2n\pi r_i} \cdot \sin\alpha + \frac{I}{2n\pi r'_i} \cdot \sin\alpha' \tag{7}$$

The conductor's cross section of geometric shape, as shown in **Figure 2**, introduces another variable into the calculations, namely that when changing the coordinate $x$, the thickness $t$ also modifies the value of the hypothetical conductor radius $R_{(fx)}$. After dividing the inductor conductor into $n$ elementary conductors, through each one of which an $n$th share of the total current $I$ passes, $I_n = I/n$. The radius of each of these conductors $R_{(fx)}$ will be a function of $x_i$ or $i$. The magnetic field intensity $H_{x_i}$, which is acting on the surface at a point at a distance $x_i$ from the perpendicular drawn from the hypothetical conductor on the liquid metal, can be computed from the value of current $I_n$ passing through the particular elementary conductor, using the following equation:

$$H_{xi} = \frac{I}{n\pi} \cdot \frac{\sqrt{\left(R_{(fx)i} + a\right)^2 - R_{(fx)i}{}^2}}{\left(R_{(fx)i} + a\right)^2 - R_{(fx)i}{}^2 + x_i^2} = \frac{I}{n\pi} \cdot \frac{\sqrt{a^2 + 2aR_{(fx)i}}}{a^2 + 2aR_{(fx)i} + x_i^2} \tag{8}$$

At a common point on the surface at the $x$ coordinate and with different values of $R$, the total value $H_x$ will be the sum of the $n$ additions $H_{x_i}$ from all $n$ elementary conductors and their $n$ mirror images, that is,

$$H_x = \sum_{i=0}^{i=n} \frac{I}{n\pi} \cdot \frac{\sqrt{a^2 + 2aR_{(fx)i}}}{a^2 + 2aR_{(fx)i} + x_i^2} \tag{9}$$

The relation $N = H^2/2\delta\sigma$ [15] describes the power generated under the surface of a specific unit area in a volume of great depth, where $\sigma$ is the electrical conductivity of liquid metal (S m$^{-1}$), $\delta = \sqrt{1/\mu\sigma\pi f}$ is the depth under molten metal surface at which the magnetic field intensity decreases $e$ times and is termed "skin depth" (mm), and $f$ is the frequency (Hz). Looking at Eq. (6), we can see the pressure developed by the magnetic field varies linearly with the value $H^2$. If we substitute the quantity $H$ from Eq. (6) into the formula for the power produced $N = H^2/2\delta\sigma$, we get

$$N = \frac{H^2}{2\delta\sigma} = \frac{2g\rho h}{\mu\sigma\delta} = 2g\sqrt{\frac{\pi}{\mu}}\,\rho h\,\sqrt{\frac{f}{g}} \tag{10}$$

Eq. (10) determines the value of the power supplied by the inductor at the unit area of the molten metal surface, which depends on the height of the molten metal column. It represents

conditions of equilibrium between the power of the magnetic field and the metallostatic pressure, taking physical properties (the electrical conductivity $\sigma$ and the density $\rho$) of the liquid metal, and also the frequency $f$ into consideration. The alternating magnetic field performs only negligible mechanical work, and by way of induced currents, almost all the energy is transmitted to the slab as heat, where the power $N$ in watts is numerically equal to the quantity of the generated heat $Q$ in J $s^{-1}$.

Taking the active power $N$ as a criterial quantity to determine the equilibrium conditions between the mechanical and electric quantities for the liquid metal levitation can be considered the very applicable decision. It provides the correct information about the amount of heat required for the thermal analysis and eliminates substantially the need for measuring the electric quantities, as voltage and the electric current in an inductor, its inductance, the finding cos $\varphi$, and the challenging calculations. As it follows from Eq. (10), at the given physical properties of liquid metal and a height of the molten metal column $h$, the power required to generate the levitation will be directly proportional to the square root of the working frequency.

## 3. Role of operating frequency of EMM

After entering the liquid metal, the alternating magnetic field induces an electrical current in it, which generates its own magnetic field, but the opposite one. As a result, the field decays exponentially when penetrating, and both interacting fields produce the force acting in the liquid metal in the direction from the inductor. At any depth $z$, in every element of the volume having an area of $1 \times 1$ $m^2$ and the depth $dz$, the increase of force $d\boldsymbol{f}$ arises, and is numerically equal to the increase in the pressure $dp$ (N $m^{-2}$). At any depth $z$ under the surface, we calculate the total value of pressure $p_m$ using the integration of all the additions in an interval from the surface, where $z = 0$, to the depth $z$, when we get [4, 16].

$$p_m = \int_0^z \left(\frac{\mu H^2}{2\delta}\right) e^{-2z/\delta} dz = \left(\frac{\mu H^2}{4}\right) \left[e^{-2z/\delta}\right]_0^z \tag{11}$$

If $z = \infty$ (or $z > 3\delta$) then $\exp - 2z/\delta$ approaches 1, and the expression of $p_m$ is identical with the expression for electromagnetic force in Eq. (6). As follows from the principle of generation of electromagnetic forces, they do not act on the surface itself but arise in the subsurface layer, on which the surface is supported. The center of their action lies at the depth $z_c$, which divides the molten metal volume into two parts in which an equal portion of the total pressure is created. According to Eq. (11), 50% of the generated pressure will be acting in the subsurface layer, where $\exp - 2z_c/\delta$, thus $z_c \approx 0.3466\delta$. At this depth, the surface is supported and, therefore, the operating frequency of the current flowing through the inductor is the important parameter [7, 17]. The frequency needs to be both high enough so that the surface layers do not flow vertically down from the faces of the shaped liquid metal, and as low as possible because any increase also increases electric energy consumption. Therefore, during shaping of a radial profile, surface tension forces are always involved. These, together with the electromagnetic force, produce the equilibrium with the metallostatic pressure of the liquid metal column on

the molten metal surface. The surface tension $\tau$ determines that the shape of the fluctuated liquid metal on the surface is semicircular with radius $r$, in which a pressure is created which is able to overcome the metallostatic pressure produced by the molten metal column $h$. Under the gravity acceleration $g$, the equilibrium force can be written thus

$$\rho g h = \frac{2\tau}{r} \tag{12}$$

When appraising the function of the surface tension for shaping the free surface, we will start with the situation presented in **Figure 3**, which can arise when, as a result of an unintended fluctuation in the molten metal, a bulge arises on its surface, and the surface tension force forms it into a hemispherical shape. The analysis is based on model conditions when the uniform magnetic field is acting, thus ignoring the increase in its intensity caused by reducing the air gap.

At the point of the jut creation, the metallostatic pressure is balanced by the pressure developed by the magnetic field and the centers of its action lay at a depth of $0.3466\delta$ under the surface in the direction of the propagating field. The array of these centers of action has the same hemisphere shape with the radius $r_v$, equal to that of the bulge, but its center is shifted under the plane of the liquid metal at a depth of $0.3466\delta$. At the axial cross section of the bulge, the surface of the spherical cap above the liquid metal plane is shaped like an arc of a circle, at the center of which the total pressure developed by the field is acting. The center of an arc of a circle according to analytic geometry lies on its axis at a distance of $r_v t/l$ from the center where $t$ is the chord length and $l$ is the length of this arc.

Gravitational force acts on the hemisphere's center which is located at a distance greater than $3/8 r_v$ from the plane of the molten metal pool. In order to prevent the hemisphere from sliding

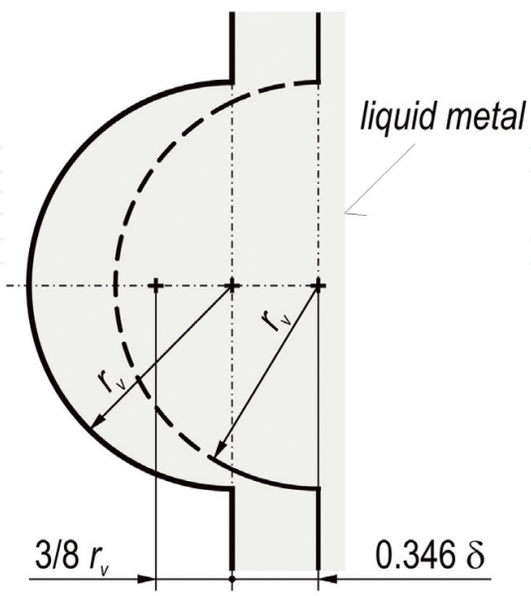


**Figure 3.** A bulge on a free surface.

in the direction of gravity, the center of the electromagnetic force acting on it has to be located at a distance greater than 3/8 $r_v$ from the molten metal plane. In a threshold situation, both centers will be identical $3/8r_v + 0.3466\delta = r_v t/l$, which is fulfilled when $r_v = 0.816\delta$. Inside the bulge the metallostatic pressure of the liquid metal column of the height $h = 2r_v$, which is in equilibrium with the surface tension force, is experienced. If we substitute into Eq. (12) for $h = 2r_v$ and the dependence $r_v = 0.816\delta$, under these conditions the centers of electromagnetic and gravitational forces have a congruent location, then the expression relating to the minimum working frequency $f_{min}$, after transforming takes the form:

$$f_{min} = 0.816^2 \frac{g}{\mu\pi} \frac{\rho}{\sigma\tau} = 1.654.10^6 \frac{\rho}{\sigma\tau} \tag{13}$$

Replacing the density $\rho$, the surface tension $\tau$, and the specific electrical conductivity $\sigma$ of the particular shaped liquid metal into Eq. (13), we can compute the lowest working frequency $f_{min}$, at which the EMM is still functional. The working frequency of the current passing through the inductor is an important parameter for EMM functioning. It has to be high enough to ensure the stability of the free surface and at the same time, as low as possible because increasing the frequency increases energy consumption.

Experiments carried out with liquid Al alloys or PbSn in the inductor with a working frequency of 10 kHz have shown that small volumes of the liquid metal placed in a ceramic crucible in the inductor's working space had a tendency to spontaneously move from side to side and their free surface to ripple. This was irrespective of whether the crucible was orientated vertically or horizontally. When increasing the pool dimension, adding more than three times the magnetic field skin depth of metal in the direction of the magnetic field penetration, a marked decline in the oscillations in the liquid metal surface could be observed. After substituting the empirical condition $d = 3\delta$ for the skin depth expression, we can determine the lowest applicable working frequency $f_d$ limited by the pool's thickness $d$, when $f_d = 2.277 . 10^6/\sigma d^2$. The working frequency of the EMM has to be higher than or equal to the highest one of the values limited by the surface tension, the minimum frequency $f_{min}$, and the dimensions of the liquid metal pool $f_d$. To introduce the dependence of the minimum pool dimension $d_{min}$ on the working frequency into the conditions defined by Eq. (10), we substitute $h = 3\delta$ for the column height. Under this condition, the value of the power density $N_d$ will be constant and proportional to the density and the specific electric resistance of liquid metal:

$$N_d = 4.684.10^7 \frac{\rho}{\sigma} \tag{14}$$

At the edge of the shaped molten metal, the surface tension creates the radius $r_\tau$, and hence in the case of the levitating molten metal pool, its height has to be $h \geq r_\tau$, because the edge radius $r_\tau$ defines the minimum possible thickness of the shaped strip $d_\tau = 2r_\tau$, which depends on the height of molten metal column $h$ and determined from the surface to the strip center [8]. For the particular alloys AlSi8.5Cu ($\rho = 2.4 \times 10^3$ kg m$^{-3}$; $\sigma = 2.56 \times 10^4$ S m$^{-1}$; $\tau = 0.865$ N m$^{-1}$) and AlSn20 ($\rho = 3.4 \times 10^3$ kg m$^{-3}$; $\sigma = 2.07 \times 10^4$ S m$^{-1}$; $\tau = 0.8$ N m$^{-1}$) [10], the conditions of the equilibrium between the power generated by the magnetic field and the level of the molten metal pool formulated in Eq. (10) are processed in **Figure 4**. The set of parameters (**Figure 4**) is

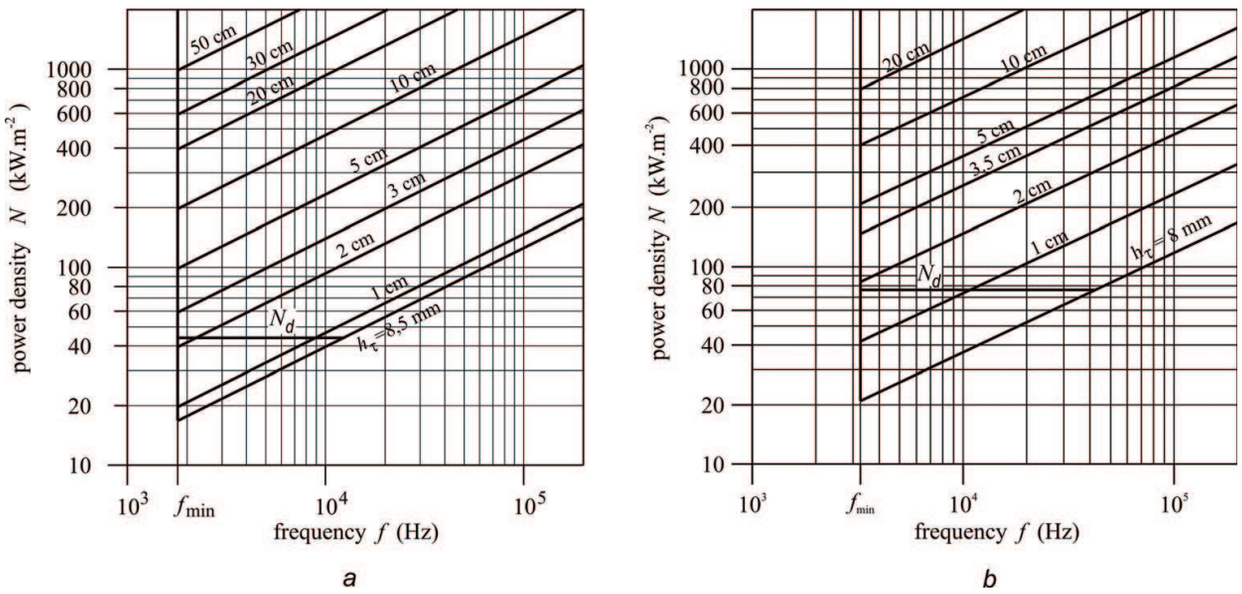


**Figure 4.** Dependence of power per area unit on a frequency at different heights of molten metal column of alloys AlSi8.5 (a) and AlSn20 (b).

limited by power of 2000 kW $m^{-2}$, because using parameters above this value entails problems with the removal of generated heat [10, 18].

In a co-ordinate system with a logarithmical scale, where the values of power density $N$ are on the vertical axis and frequency values $f$ are on the horizontal one, the conditions of the equilibrium $N$-$h$ are shown as a system of lines for the separate values of the height of molten metal column. The boundary conditions at values $r_\tau = h_\tau = h_{min}$ and $f_{min}$ are lines which limit the interval of the parameter values under which the conditions of reliable EMM performance are met. The line of values $N_d$, where the condition $h = 3\delta$ holds, allows us to read the minimum thickness of the pool $d_{\min}$ for a given frequency. For the given thickness $d$, the line of value $h = d$ intersects the line $N_d$ at the frequency $f_d$, which is the lowest value which can still be used to cast the strip of thickness $d$. Bellow the line $N_d$, at the height interval $r_\tau \leq h \leq 3\delta$, there are a range of parameters under which the performance of the vertical EMM is maintained.

## 4. Testing the horizontal inductor of rectangular cross-section

At the development of horizontal electromagnetic mould, much significance has been attached to experiments, the aim of which was to find out a dependence of magnetic field intensity $H$ on the value of a gap between the molten metal surface and the inductor in inductor's working space [10]. The experimental measurements were carried out in the inductor, which had the simple rectangle cross section of the 10 × 40 mm (**Figure 5a**). That inductor has provided a good approach to the working space when taking a measurement. In **Figure 5b**, there are presented the experimental found out courses of magnetic field intensity $H$ depending on gap's size and inductor's shape when alternating current of frequency of 10 kHz and intensity of 3200 A (rms value of 2260 A) were imposed.

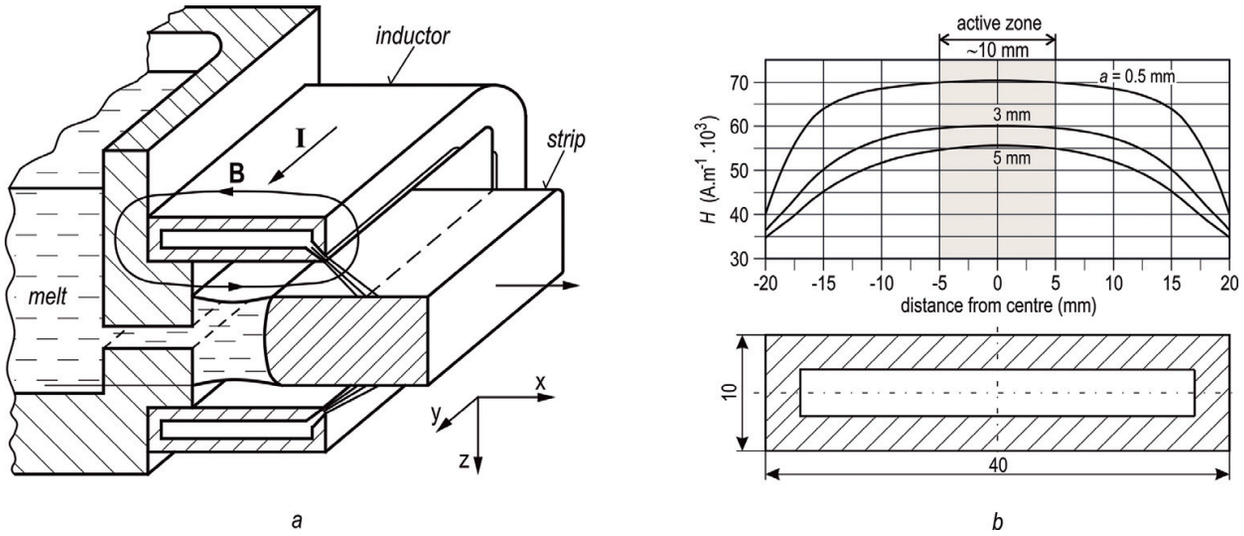


**Figure 5.** Horizontal EMM with a inductor of rectangular cross section (a) and measured magnetic field intensity $H$ under imposed alternating current of 10 kHz frequency and intensity of 3200 A (rms value of 2260 A) (b).

From the shape of curves, it is seen that inside the inductor's operating space the magnetic field is not homogenous, and at the edges, it drops markedly. Therefore, to effectively stabilize the molten metal position against the inductor, it is better to choose the smaller air gaps. Then even the small deviation in the position will cause sufficiently strong changes of magnetic field intensity, which effectively can adjust the incidental deflection of the liquid metal position produced by changes of metallostatic pressure or resulting from the movement fluctuation.

Laboratory HEMM enabled to take measurements at gap up to 10 mm, and the molten metal of the height up to 70 mm, which was kept in a corundum crucible or free levitated. Part of experimental measurements was performed under model conditions in the vertically oriented working space when the molten metal pool was supported from below by a fireclay board. The solid aluminum alloy was inserted into the inductor, and after its meltdown, the desired height of the molten metal was reached by adding an extra metal. Experimentally attained sets of $H$-$a$ values have provided data for next analytic works and development of expression which enable to determine the value of $H_x$ at any point of the molten metal surface having $x$-coordinate:

$$H_x = \sum H_i = \frac{I}{n\pi} \sum_{x=-\frac{xn}{b}}^{\frac{xn}{b}-n} \frac{\sqrt{a^2 + 2aR}}{a^2 + 2aR + \left(\frac{b}{n} i\right)^2} \tag{15}$$

A plain shape of the inductor enabled to substitute the variable $x$ for multiple of a length of the molten metal surface part being of the length $b/n$; then, $x_i = ib/n$, when $i$ is integer. The performed experiments have shown that accuracy of calculation $H_x$ for the individual gap values at dividing $n \geq 100$, and the defined geometric shape of the inductor depends namely on the accuracy of determining the value of alternating current intensity and on a method of gap measurement, because the surface of the levitated molten metal rippled moderately having an amplitude approximately ±0.5 mm.

Using the liquid AlSi8.5Cu1 alloy, for the gap of 3 mm being calculated under the rms current of 2260 A, there was experimentally measured the value of approximately 3–3.2 mm. Differences between the calculated and measured values did not exceed 10%. A validation has shown there is not necessary to use a visual assignment of values from experimentally attained curves *H-a*. It is more advantageous to employ the accurate calculation of *H-a* values which is based on interactions between the inductor and its mirror image known from the theory of induction heating [11, 12] and electromagnetic forming [19].

Based on experiments which were aimed at determining the lower power limit of the EMM and HEMM parameters, the hypothesis was developed that the fundamental limiting factor is the internal motion in the liquid metal produced by the non-potential action of the electromagnetic forces which would inevitably impact on the primary structure formation [20]. To verify this assumption, an experiment was carried out where in the vertical-oriented inductor a cone of Al alloy was melted down on a thermo-insulating insert, the center of which was cooled by immersing a water-cooled copper pipe of outer diameter of 10 mm and bent to form an arch with a radius of 20 mm. After stabilizing the heat balance, most of the liquid metal was solidified and after switching off the device, the block of solidified metal containing the cooling pipe was taken out of the inductor.

As shown in **Figure 6**, at the edge of the sample adjacent to the inductor where the cooling rate was the lowest, and however, where the level of the effect from the alternating magnetic field and the electric current flow was the highest, the gradual transition of an eutectic morphology from finely dispersed at the edge to the typical dendritic structure on the length corresponding to the skin depth $\delta$ can be observed.

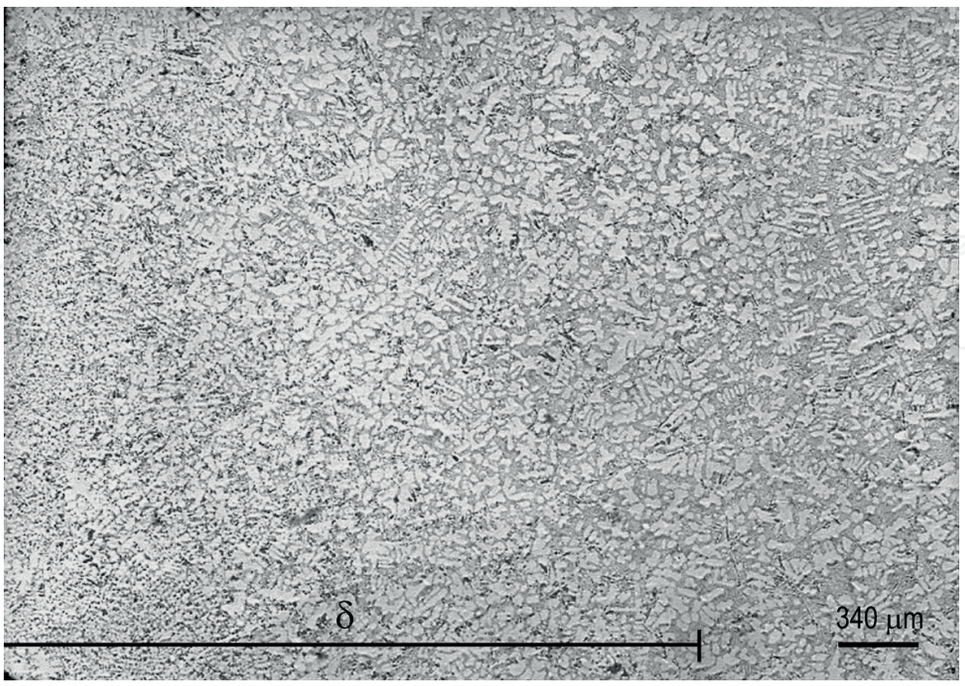


**Figure 6.** Microstructure of the AlSi8.5Cu alloy from the sample's edge to a distance of 1$\delta$.

The structure consists of fine dendrites of the primary solid solution with no clear orientation. Under the surface at a depth greater than $\delta \approx 3.2$ mm, the microstructure is almost the same as was found over most of the section in central zones of the sample. It consists of the primary solid solution and eutectic ($\alpha$ + Si) of the transition morphology type. The fact that more marked changes in the morphology occur only at a distance about the skin depth $\delta$ from the surface, can most likely attributed to the internal motion in the subsurface layer.

## 5. Design of industrial horizontal EMM

Experiments [9, 10] conducted with the laboratory HEMM comprising one coil inductor having a conductor section of 10 × 40 mm for casting the profile of 150 × 20 mm, as illustrated in **Figure 5a**, proved the feasibility of electromagnetic shaping the strip in the horizontal arrangement. The unit was powered by a generator intended for ultrasonic application with a power output of 10 kW and operating frequency of 10 kHz. The inductor used was characterized by a high drop in the magnetic field intensity in the direction away from central zone, and levitation of the liquid metal could be produced over a length of ±5 mm from the center (**Figure 5b**). At a larger distance, the free surface of the liquid metal rippled uncontrollably [9, 10].

The experiments carried out have shown that this length of active zone, provided by such an inductor, while being adequate for levitation generated by the uniform alternating magnetic field, was at the limit of application. It was evident that to extend the zone of active shaping in the direction of the exiting strip would be most easily achieved by enlarging the inductor, but such a solution would entail an increase in energy consumption. Therefore, the research was focused on the problem of how to extend the levitation zone without enlarging the inductor. Changing the wire cross section from a simple rectangular shape (**Figure 5**) to a more complex shape (**Figure 2**) was proved to be the solution.

The next step in the development of a HEMM prototype highlighted the group of problems which have to be worked out before the prototype can be tried under production conditions. These include determining the boundary parameters of the shaping process, the air gap size, and at both horizontal surfaces the edge radiuses of the shaped strip, and with respect to the different conditions of shaping of the upper and lower surfaces of strip, devising the suitable engineering designs of the inductor [21]. Two designs of inductors capable of shaping the lower and upper surfaces, together with the distribution of the magnetic field, are presented in **Figure 7**.

Research undertaken with the laboratory HEMM with the inductor of a 10 × 40 mm section has shown the solidification zone has to be located in the distance of ±10 mm from the middle, where the value of the air gap is changed about 1 mm. The difference in air gap values from 20 to 21 mm above the upper surface was chosen to ascertain over what length of the inductor in the direction of exiting it is possible to keep this range of air gaps. From the distribution of the magnetic field intensity (**Figure 7b**), it follows that at the nominal value of magnetic field intensity of 32 kA $m^{-1}$, the arrangement with auxiliary inductors placed 6 mm below the main inductor ensures that the air gap will be ranged from 20 to 21 mm ($a_1$ = 8 and 9 mm) between

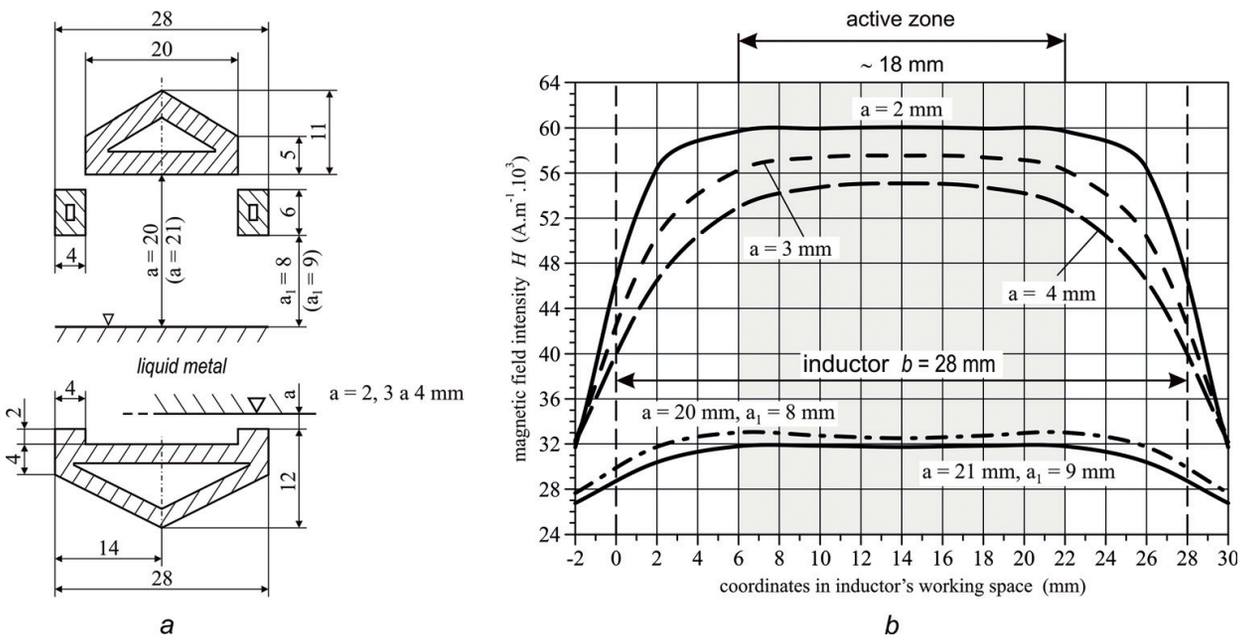


**Figure 7.** Arrangement of inductors for shaping of both surfaces (a), and the distribution of the magnetic field at an electric current of a peak value of 2520 A (b).

coordinates of 2 and 26 mm, which means over the length up to 24 mm. Over this interval, the internal movements of molten metal will be only negligible. Positioning an auxiliary inductor at the outlet makes it possible to locate a barrier directly at the edge of the working space of the inductor to prevent water entering into the solidification zone. It can be a curtain, baffle or roller, made from silicon rubber. The design can be seen as successfully developed and was used as the universal solution to shaping the upper surface of the strip, while the total width of 28 mm became the standard for inductors intended for the lower surface shaping.

The configuration of the inductor, which is intended for shaping a strip's lower surface, is also based on generating additional intensity of the magnetic field through the use of two auxiliary inductors which are integrated into one unit with the main inductor. **Figure 7a** shows the cross section of the inductor which has 2 mm raised edges, together with the distribution of its magnetic field intensity at air gap values of $a$ = 2, 3, and 4 mm at the raised edges (**Figure 7b**). For every value of $a$ = 2, 3, and 4 mm at the edge, the values of the air gap at the central plane of the inductor are about 2 mm higher, hence the distance of inductor's central part from the surface of the molten metal will be 4, 5, and 6 mm. On the lower surface with a magnetic field intensity of 56 kA $m^{-1}$, a satisfactory stability of molten metal can be expected between coordinates of 2 and 26 mm, that is, over the length of 24 mm, where the air gap $a$ will range from 2 to 4 mm. Under working conditions, it is desirable to locate the solidification zone $l/s$ in the interval between coordinates 6 and 22 mm of the inductor's width in between the auxiliary inductors. It is possible to extend the interval to the $x$ coordinate of 4 mm, which will result in increasing the strip's thickness by about 1 mm, or up to the $x$ coordinate of 2 mm, when the strip's thickness will rise to approximately 1.6 mm, whilst retaining the functionality of the HEMM.

Both design arrangements, which meet requirements for the industrial use of the HEMM, are presented in **Figure 8** with a tank of molten metal. In **Table 1**, the HEMM's parameters for continuous casting of a 20 mm thick strip of AlSi8.5Cu and AlSn20 alloys are listed.

The raised edges of the HEMM's working space, which ensure a proper distribution of the magnetic field in the lower surface of the strip, also form a channel from which the cooling water splashed from the cooling system or condensed on the inductor has to be drained. Similarly at the end of the casting process, when the liquid metal no longer exerts a lifting force, the channel serves to drain the surplus molten metal. A steady run-off of water can be ensured by the gentle 1–2° slope of the HEMM or can be created with a sloped surface from

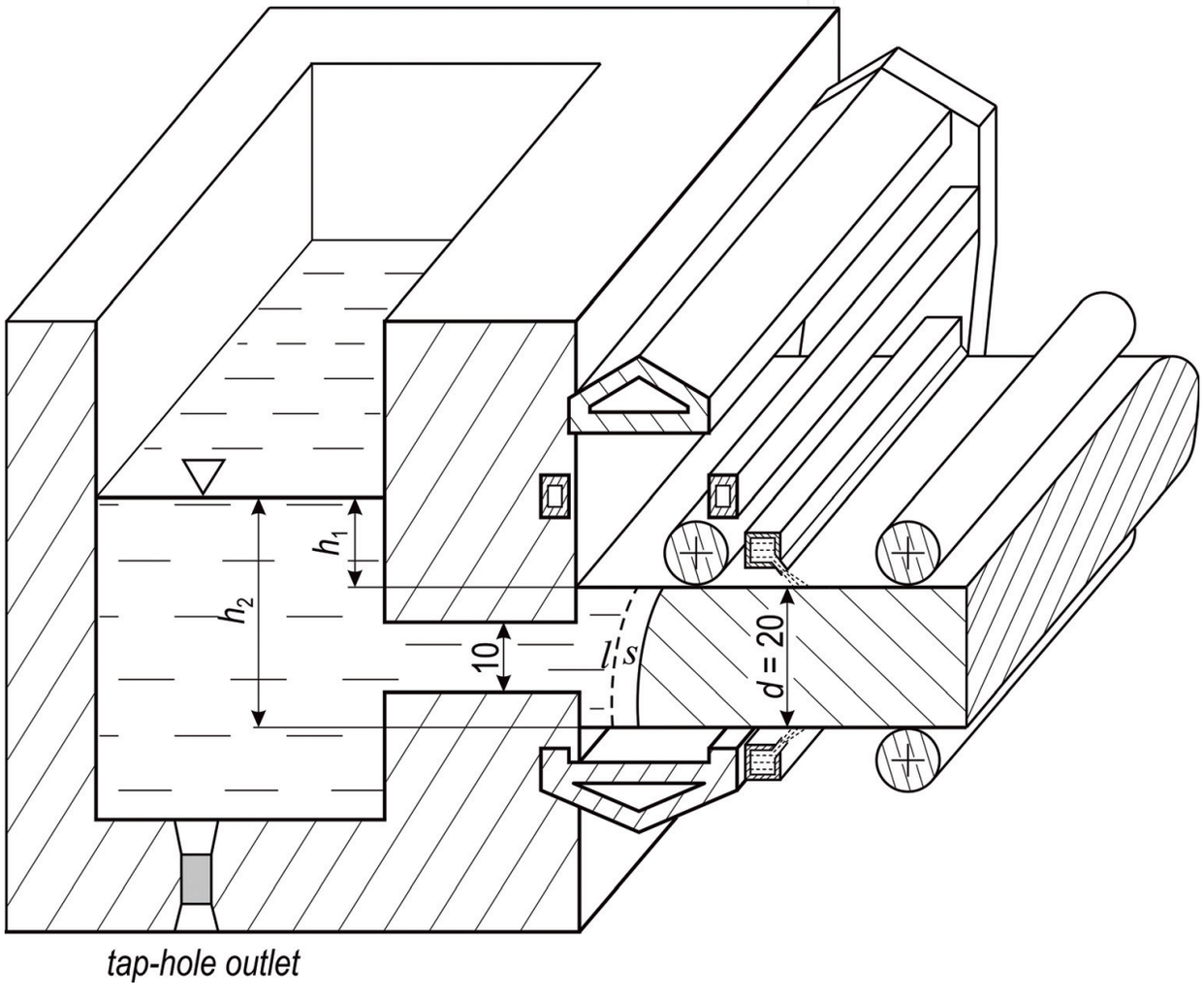


**Figure 8.** Arrangement of the HEMM unit for continuous casting of a 20 mm thick strip from Al alloys.

| Material | $H_2$ (kA m$^{-1}$) | $h_2$ (mm) | $H_1$ (kA m$^{-1}$) | $h_1$ (mm) | $\Sigma Q$ (J s$^{-1}$) | $I_{ef}$ (A) | $\delta$ (mm) | $\rho$ (kg m$^{-3}$) |
|---|---|---|---|---|---|---|---|---|
| AlSi8.5Cu | 47.32 | 29.83 | 27.04 | 9.76 | 879 | 1507 | 3.17 | $2.4 \times 10^3$ |
| AlSn20 | 56.30 | 29.84 | 32.16 | 9.74 | 1282 | 1791 | 3.26 | $3.4 \times 10^3$ |

**Table 1.** Parameters of horizontal EMM for continuous casting of Al alloys.

organosilicate or moister-proof ceramics over the whole width of the inductor to the lateral gap. The slope area could also function as an emergency run-off for the liquid metal.

One of the technological features of the HEMM, as seen in **Figure 8**, is the distinct positioning of a cooling zone for both the upper and lower surfaces. Values for the intensity of the magnetic field of 47.32 and 27.04 kA $m^{-1}$, when shaping a 20 mm thick strip of AlSi8.5Cu alloy in the inductor (**Figure 7a**) with current $I$ flowing at 2132 A ($I_{ef} = I\sqrt{2} = 1507$ A), correspond to 139 kW $m^{-2}$ of power density generated at the upper surface, and to 46 kW $m^{-2}$ at the lower surface, according to **Figure 4** and Eq. (10). When the AlSn20 alloy is shaped with current $I$ = 2533 A ($I_{ef}$ = 1791 A), the magnetic field intensity of 56.28 and 32.16 kA $m^{-1}$ correspond to values of the generated power density of 204 and 66 kW $m^{-2}$, respectively. Better conditions for the heat removal and less intensive induction heating of the upper surface result in the solidification zone being about 4–5 mm closer to the outlet in the upper part than in the lower one. Analysis of temperature conditions [18] has shown that axial heat removal will prevail, isosolidus of which has a shape indicated in **Figure 8**. This creates the adequate conditions for directional solidification and additional feeding when compensating for the loss of volume during solidification. In order to finish the process of continuous casting, it is necessary to reduce the level of or completely to evacuate the liquid metal from the tank as quickly as possible. This reduces to a minimum the end segment of the continuous cast strip having a reduced thickness.

At this point, it is necessary to understand that if the height of the levitating molten metal falls below 10 mm, then the pool will disintegrate as a consequence of its internal movement. From a technological point of view, the most favorable method for evacuating the tank is by "tapping," that is, by creating an opening in its bottom which is filled with for example clay bonded moulding sand, through which the molten metal can be channeled into a collecting crucible. Breaking an opening has to involve simultaneous cutting off of the supply of liquid metal to the tank. It follows that at the expected withdrawal speed of 1.5 m $min^{-1}$, the strip covers the distance of 10 mm between the solidification zone and the area of the strongest cooling in 0.4 second, and the whole length of the working space between the tank lining and the outlet plane of the inductor in approximately 1 s.

The inductor in the form as seen in **Figure 8** enables the solidification zone to be located on the upper surface only approximately 3 mm from the inductor's edge, and the cooling zone to be close to the edge. This is possible because under the auxiliary inductor, there is ample space to put a roller, curtain, or baffle to prevent the water leaking into the operating space. On the lower surface, the conditions are more complicated because the small gap enables the zone of strong cooling to be located 2–3 mm in front of the face of the inductor, and the solidification zone then has to be at least 5.5 mm behind the inductor's face. In this case, the distance between the solidification and cooling zones will be 7.5–8.5 mm or, with some allowance, 10 mm. Determining a speed of withdrawal was the subject of research [18] which has pointed out the crucial effect of three factors: the efficiency of cooling of the shaped strip by water spraying; the amount of Joule heat produced in the process of shaping; and the positioning of the solidification zone being limited by the magnetic field distribution. Work [18] states that when pouring AlSi alloy it is possible to achieve an exit speed up to 2.0 m $min^{-1}$ when the area

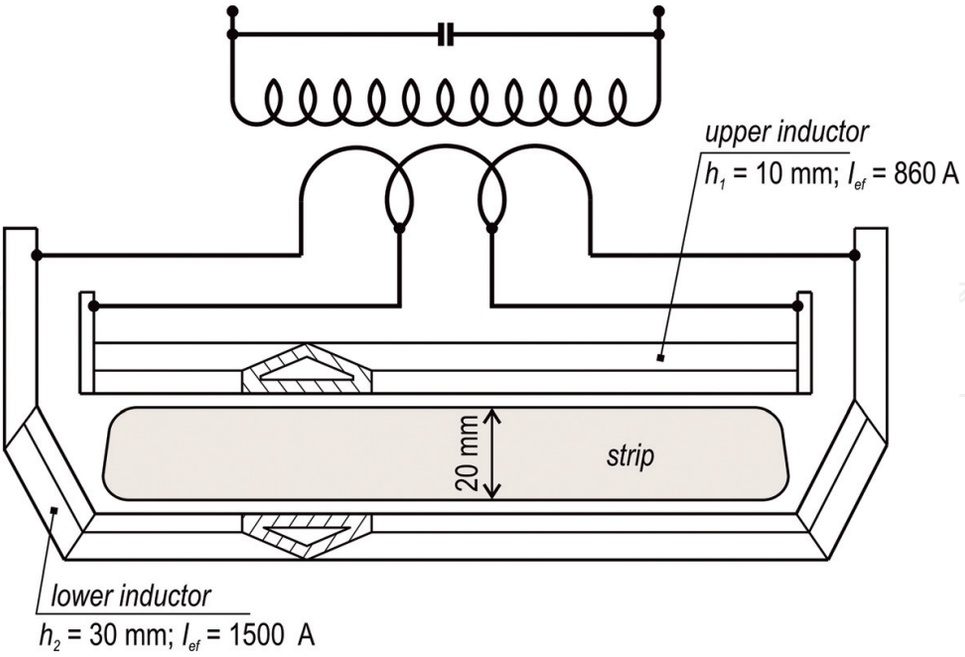


**Figure 9.** Horizontal EMM consisting of two separate inductors connected parallel for shaping a strip of 20 mm thickness.

of optimal bilateral cooling of the strip is 10 mm away from the solidification zone, and with certain allowance, a speed of about 1.5 m $min^{-1}$ can be achieved for common cooling.

Another possible concept of the horizontal electromagnetic inductor is presented in **Figure 9**. The devised electromagnetic mould consists of two separate inductors with the same cross section of a base, the upper and bottom ones, which are connected parallel and passed with the electric current of different intensities [22]. This requirement can be assured by the separated feeding of the both inductors, or by connecting a shunt to the upper inductor. Applying an air gap of 2–6 mm for both peripheries of the strip, the inductor confining the bottom surface has to be passed by the substantially higher current of 1500 A than the upper inductor that is passed by 860 A.

## 6. Conclusions

The horizontal EMM is a promising technical instrument, the development of which has already reached a stage when it is possible to expect its adoption by industry. When undertaking the research, the author based it on a critical analysis of a prototype unit and primarily on the design of a laboratory inductor, which enabled the experiments with the HEMM to be carried out, and provided crucial suggestions for the design of an industrial unit prototype. The theoretical analyses supported by the extended experimental work has shown that conditions for confining and shaping the upper and bottom surfaces of liquid metal required the distinct spatial arrangement of inductors. The presented way of designing the electromagnetic moulds is based on the analysis of effects of changes in inductor's shape on the magnetic field distribution and subsequent targeted use of inductor's shape adjustment.

## Acknowledgements

The author appreciates the financial support provided by Slovak Research and Development Agency for the projects APVV-0857-12 and APVV-16-0485.

## Author details

Marcela Pokusová

Address all correspondence to: marcela.pokusova@stuba.sk

Faculty of Mechanical Engineering, Slovak University of Technology in Bratislava, Bratislava, Slovak Republic

## References

[1] Getselev ZN. Casting in an electromagnetic field. Journal of Metals. 1971;**23**(10):38-39. DOI: 10.1007/BF03355734

[2] Yoshida M. Electromagnetic casting up to date and future. Tetsu-to-Hagane. 1987;**73**(3): 403-410. DOI: tetsutohagane1955.73.3_403

[3] Zhu XR, Harding RA, Campbell J. Calculation of the free surface shape in the electromagnetic processing of liquid metals. Applied Mathematical Modelling. 1997;**21**(4):207-214. DOI: https://doi.org/10.1016/S0307-904X(97)00008-5

[4] Sakane J, Li BQ, Evans JW. Mathematical modeling of meniscus profile and melt flow in electromagnetic casters. Metallurgical Transactions B. 1988;**19**(3):397-408. DOI: 10.1007/BF02657737

[5] Lavers JD. Computational methods for the analysis of molten metal electromagnetic confinement systems. ISIJ International. 1989;**29**(12):993-1005. DOI: http://doi.org/10.2355/isijinternational.29.993

[6] Roche JR, Canelas A, Herskovits J. Shape optimization for inverse electromagnetic casting problems. Inverse Problems in Science and Engineering. 2012;**20**(7):951–972. DOI: http://dx.doi.org/10.1080/17415977.2011.637206

[7] Ren Z, Deng K, Zhou Y, Zhu S, Jiang G. Basic study of horizontal electromagnetic levitation casting of aluminum sheet. ISIJ International. 1996;**36**:S194-S196. DOI: http://doi.org/10.2355/isijinternational.36.Suppl_S194

[8] Murgas M, Pokusova M. Electroamgnetic crystallizer for continuous casting the AlSi8.5 alloy strip. Solidification of Metals and Alloys. 1997;**33**:20

[9] Pokusova M, Murgas M. Horizontal electromagnetic caster for continuous casting of the Al-alloys. In: Electromagnetic Processing of Materials; 26–29 May 1997; Paris-la-Defense. Paris: Centre Francais De L'Electricite; 1997. pp. 73–78

[10] Pokusova M. Electromagnetic Processing of Aluminium Alloys. 1st ed. Trnava: AlumniPress; 2007. p. 100

[11] Brown GH, Hoyler CN, Bierwirth RA. Induction Heating Handbook. New York: D. Van Nostrand Company, Inc.; 1947. p. 370

[12] Langer E. Theory of Induction and Dielectric Heat. Praha: Academia; 1964. p. 291

[13] Vives C, Ricou R. Experimental study of continuous electromagnetic casting of aluminium alloys. Metallurgical Transaction B. 1985;**16B**(2):377-384. DOI: 10.1007/BF02679730

[14] Yamane H, Bhamidipati JR, El-Kaddah N. Analysis of electromagnetic confinement and solidification of a vertical molten metal sheet in electromagnetic strip casting. In: International Symposium on Electromagnetic Processing of Materials—EPM94. 25 – 28 October 1994; Nagoya. Tokyo: The Iron and Steel Institute of Japan; 1994. p. 35-40

[15] Asai S. Birth and recent activities of electromagnetic processing of materials. ISIJ International. 1989;**29**(12):981-992. DOI: 10.2355/isijinternational.29.981

[16] Zhang Z, Xun J, Shi L. Study on multiple electromagnetic continuous casting of aluminum alloy. Journal of Materials Science & Technology. 2006;**22**(4):437-440

[17] Nakata H, Etay J. Meniscus shape of molten steel under alternating magnetic field. ISIJ International. 1992;**32**(4):521-528. DOI: http://doi.org/10.2355/isijinternational.32.521

[18] Taraba B, Behulova M. Modelling of the continuous casting of pure aluminium in electromagnetic crystallizer. In: CO-MAT-TECH 93; 26–27 October 1993; Trnava. Trnava: STU in Bratislava; 1993. pp. 148–150

[19] Xu D, Xuesong L, Fang K, Fang H. Calculation of electromagnetic force in electromagnetic forming process of metal sheet. Journal of Applied Physics 2010;**107**:124907. DOI: http://dx.doi.org/10.1063/1.3437201

[20] Shen J, Li J, Fu H. Electromagnetic confinement and shaping for plate-form part. Journal of Materials Science & Technology. 2000;**16**(1):27-32

[21] Pokusova M, Murgas M. Using electromagnetic levitation for continuous casting of thin aluminium alloys strip. ISIJ International. 2015;**55**(8):1669–1676. DOI: http://dx.doi.org/10.2355/isijinternational.ISIJINT-2014-843

[22] Pokusova M, Murgas M, Tehlar P. Method of horizontal continuous casting of metals and assembly inductors of horizontal electromagnetic crystallizer. Slovakia; Patent application No. SK50272015 (A3), 2017

IntechOpen

IntechOpen